Microcirculation (2000) 7, 269–280

www.nature.com/mn

Effects of Myocardial Edema on the Development of Myocardial Interstitial Fibrosis

K.L. DAVIS,* G.A. LAINE,*‡ H.J. GEISSLER,† U. MEHLHORN,† M. BRENNAN,* AND S.J. ALLEN*

*Center for Microvascular and Lymphatic Studies, Department of Anesthesiology, The University of Texas–Houston Medical School, Houston, TX, USA; and †Clinic for Cardiovascular Surgery, University of Cologne, Germany; and ‡Michael E. DeBakey Institute for Comparative Cardiovascular Science, Texas A&M University, College Station, TX, USA

ABSTRACT

Objective: The mechanism by which chronic myocardial edema causes cardiac dysfunction is poorly understood. We hypothesized that myocardial edema triggers cardiac fibrosis development resulting in cardiac dysfunction. Since collagen is the most abundant constituent of the interstitial matrix, we examined the effects of edema development on cardiac collagen metabolism.

Methods: We utilized a chronic pulmonary artery banded rat model that produces right ventricular hypertrophy with myocardial edema and left ventricular edema without hypertrophy or hyperplasia. Wet to dry ratios (index of edema), collagen type I and III concentrations, prolyl 4-hydroxylase (P4-H) and collagen type I and III mRNA levels, collagenase activity and transforming growth factor-β were measured in both ventricles.

Results: Right and left ventricular wet to dry ratios were significantly elevated from 1 to 28 days after pulmonary artery banding compared to sham rats. Right and left ventricular collagen types I and III and P4-H mRNA levels increased significantly at 3 days followed by significant increases in right and left ventricular collagen concentration 7 days after pulmonary artery banding. Right ventricular collagenase activity increased at 3 days while left ventricular collagenase activity decreased 7 days after PA banding.

Conclusions: We conclude that myocardial edema preceded the observed increase in collagen deposition and that edema may have triggered increased collagen synthesis by fibroblasts, leading to fibrosis development. **Microcirculation (2000) 7, 269–280.**

KEY WORDS: myocardial edema, cardiac fibrosis, collagen, collagenase, interstitium, prolyl 4-hydroxylase

INTRODUCTION

Myocardial edema has been shown to develop and cause left ventricular (LV) dysfunction in several diseases including pulmonary hypertension, systemic arterial hypertension, right heart disease, and during cardioplegic arrest (10,17,21,28,29). The mechanism by which edema causes this cardiac dysfunction is poorly understood. Acute interstitial myocardial edema has been shown to have a direct negative impact on cardiac function (10,17,21). Chronic myocardial edema has also been shown to impair cardiac function but the mechanism is unclear (17). Chronic myocardial edema may have both a direct impact on cardiac function and an indirect effect on cardiac function by triggering interstitial fibrosis development. The impact of myocardial edema on cardiac fibrosis development has not been thoroughly studied.

There is evidence to suggest that LV fibrosis can cause LV dysfunction. In experimentally induced ar-

Supported by National Heart, Lung, and Blood Institute Grant No. HL-36115 and the American Heart Association.
For reprints of this article, contact Dr. Glen A. Laine, Director, Michael E. DeBakey Institute, Texas A&M University, College Station, TX 77843-4466, USA; e-mail: glaine@tamu.edu
Received 26 January 2000; accepted 4 April 2000

terial hypertension, an increase in collagen content resulted in an increased LV chamber stiffness (5). Similarly, when LV fibrosis was induced by LV pressure overload in primates, both systolic and diastolic dysfunction were observed (41). Abnormal LV chamber stiffness was also observed in a cardiac fibrosis model in which LV collagen remodeling was induced in rats in the absence of hypertrophy (25). As myocardial edema is often associated with myocardial interstitial fibrosis development and myocardial fibrosis has been shown to cause cardiac dysfunction, myocardial fibrosis may be partially responsible for the cardiac dysfunction observed in chronic myocardial edema. The purpose of this study was to investigate the effects of myocardial edema on cardiac fibrosis development including collagen synthesis, processing, and degradation in a chronic myocardial edema model. The concept that chronic edema causes an increase in extracellular fibrotic tissue is not new. In early studies of the lymphatic system, chronic obstruction of lymph flow from tissue was described as causing "excessive laying down of connective tissue" (22). When chronic impairment of lymph flow from the heart was produced by ligation of the efferent cardiac lymphatics, increased elastic and fibrous tissue in the LV endocardium were observed (22,38). Furthermore, interstitial fibrosis is often associated with edema in other organs. Pulmonary fibrosis is frequently associated with pulmonary edema (33) and peripheral fibrosis is often associated with systemic lymphedema (44). The presence of increased myocardial interstitial fibrosis in the hypertrophied human heart has been well documented (14,27,31,32,35,40). In a previous study, we demonstrated that both myocardial edema and myocardial interstitial fibrosis exist as confounding factors associated with chronic congestive cardiomyopathy in humans (43).

To study the effects of edema on fibrosis development, we chose a chronic pulmonary artery (PA) banded rat model. In this model, pulmonary hypertension (PH) has been shown to induce myocardial edema in both the right and left ventricles (17). The LV becomes edematous for two reasons. First, elevation of PA pressure leads to increased right ventricular (RV) and right atrial (RA) hydrostatic pressures, because LV venous drainage enters the RA through the coronary sinus, pressure in the coronary sinus is increased and left ventricular microvascular exchange vessel pressure is elevated, resulting in increased transmicrovascular fluid flux and left ventricular edema formation. Secondly, as elevation of PA pressure results in right-sided pressure elevations (right ventricular, right atrial, and central venous pressure), and as cardiac lymph drains into the central venous system, the rate of removal of edema fluid from the LV via the cardiac lymphatics is decreased, thus further exacerbating LV edema formation (18,42).

The RV is subjected to pressure overload and subsequently develops hypertrophy; however, the LV does not experience any significant hemodynamic perturbations. We can, therefore, study the effects of myocardial edema on fibrosis development in the LV in the absence of pressure overload and hypertrophy. Although we studied fibrosis development in both ventricles, we chose to focus on the LV to study the effects of edema. Since collagen is the most abundant protein in the extracellular matrix, we measured collagen accumulation as an indicator of fibrosis development in our model. We focused on several levels in the process of collagen accumulation including total collagen content, collagen mRNA levels, prolyl 4-hydroxylase mRNA levels involved in collagen processing, and collagenase activity.

MATERIALS AND METHODS

Experimental Protocol

Male Sprague-Dawley rats weighing between 325–400 g were used. All procedures were approved by the University of Texas Medical School Care and Use Committee and were consistent with the NIH *Guide for the Care and Use of Laboratory Animals.* Anesthesia was induced with the inhalation anesthetic halothane. The rats were intubated and mechanically ventilated with an air–halothane mixture to maintain anesthesia (Harvard Rodent Ventilator Model 683; Harvard, Southnatick, MA). A fluid-filled catheter was placed in the femoral artery to monitor mean arterial pressure and a median sternotomy was performed. After the PA was dissected from the aorta, a 16G luer stub adapter was placed along the PA and a ligature was tied tightly around both the PA and the adapter. The adapter was quickly removed leaving the ligature around the PA. This produced a PA constriction of the same diameter in each rat. As a PA catheter is difficult to place in rats, right ventricular pressure (RVP), reflecting changes in PA pressure, was measured by placing a 27G needle attached to a fluid-filled catheter directly into the right ventricle. The femoral artery and RV catheters were connected to pressure transducers (Healthdyne Isotec disposable, Irvine, CA). Data was displayed and acquired using a Maclab 8 channel data acquisition system (World Precision Instruments, Inc., Sarasota, FL) and a

Macintosh computer (Macintosh Quadra 700, Apple Computer, Inc.). Following RVP measurement, the sternotomy was closed and the rat was allowed to recover. Gentamicin (0.5 mg/kg per day) was given for three days starting on the day of the surgery to prevent infection. Control rats were subjected to the same surgical protocol except the PA was not banded (sham operated).

After 0, 1, 3, 7, or 28 days of pulmonary hypertension, rats were reanesthetized and the sternum was opened to measure RVP again. The rats were then sacrificed by injecting a bolus of saturated KCl into the heart while still under anesthesia. Following sacrifice, the right ventricle and left ventricular free wall (not including the septum) and the biceps femoris muscle were excised for determination of wet to dry ratio, collagen content, collagen and prolyl 4-hydroxylase mRNA levels, or collagenase activity.

Myocardial Edema

To determine the amount of myocardial edema accumulation, wet to dry ratios were measured at 0, 1, 3, 7, and 28 days after PA banding or sham operation. The amount of myocardial edema was determined using a gravimetric wet to dry ratio where (wet weight – dry weight)/dry weight is the wet to dry ratio (17,26). A blood correction was not performed due to the small sample size. Wet to dry analyses were also performed on the biceps femoris muscle of sham and PA banded rats.

Collagen Content

At the time of sacrifice (0, 1, 3, 7, or 28 days after surgical procedure), the excised heart was separated into right and left ventricles and rinsed in cold water to remove blood. Samples of skeletal muscle (biceps femoris) were also collected for collagen determination. The samples were homogenized, then dried until no change in weight could be detected. Each sample was assayed in duplicate.

Total collagen was measured using a hydroxyproline colorimetric assay as described by Berg (3). This assay is a colorimetric reaction based on the oxidation of hydroxypyrrole to pyrrole, which reacts with *p*-dimethylaminobenzaldehyde (DAB) to form a chromophore. Since no proteins other than collagen contain an appreciable amount of hydroxyproline, the amount of hydroxyproline in a sample correlates very well with the amount of collagen in that sample.

This colorimetric assay was performed as follows. Four to five mg of dry tissue were hydrolyzed in 6 N HCl at 110 °C overnight. The samples were then cooled and neutralized with NaOH. Isopropanol was added to an aliquot of hydrolyzed sample and mixed thoroughly. To this isopropanol mixture, chloramine T was added and the sample was incubated 4 minutes at room temperature. Following addition of DAB, the sample was incubated at 58 °C for 30 minutes to develop color. Absorbance of the sample was measured at a wavelength of 558 nm on a spectrophotometer (LKB Ultrospec II, Upsala, Sweden). Known amounts of collagen were also assayed to obtain a standard curve (rat tail collagen type I, Sigma type VII, Sigma, St. Louis, MO). Collagen content was reported as g% (grams collagen/grams dry heart weight).

RNA Isolation

Collagen type I and III, prolyl 4-hydroxylase, and TGF-β mRNA levels were measured 1, 3, and 7 days after PA banding or sham operation. RNA was isolated from sham and PA banded rats using a procedure described by Glisin et al. and Ullrich et al. (12,39). Briefly, the RV and LV free wall were collected as described above and placed immediately into 5 M guanidine thiocyanate (GTC). The ventricles were homogenized then centrifuged to remove any particulate cellular debris. The supernatants were layered over a 5.7 M cesium chloride cushion and centrifuged for 18 hours at 25,000 *g*. The supernatants were then carefully removed without contaminating the RNA pellet. The pellets were resuspended in diethyl pyrocarbonate treated water (depc H_2O) and extracted with a 25:24:1 phenol: chloroform:isoamyl alcohol mixture. The extracts were then ethanol precipitated, resuspended in depc H_2O, and quantified spectrophotometrically (λ = 260 nm).

Electrophoresis

After RNA isolation, 10 μg of RNA were separated by electrophoresis on a 1% agarose gel containing 20% formaldehyde (2). After separation, the RNA was transferred to a Duralon membrane by electrophoretic transfer. The membranes were then subjected to Northern blot analysis. Total RNA from sham operated and pulmonary hypertensive rats were loaded on the same gels to eliminate intergel variability caused by differences in hybridization and wash conditions and differences in probe specific activity. Glyceraldehyde-3-phosphate dehydrogenase (GAPDH) mRNA levels were used to control for loading differences.

Hybridization Probes

Probes for Northern blot analysis were made by the random priming method described by Feinberg and

Vogelstein or by a riboprobe synthesis method (11,34). In the random priming method, the DNA fragment of interest was excised from the plasmid and denatured. A group of heterogeneous random oligonucleotides were used as primers in the polymerase reaction along with radiolabeled deoxyadenosine triphosphate and the Klenow fragment of *Escherichia coli* DNA polymerase I. In the riboprobe synthesis method, single-stranded radiolabeled RNA probes were made from a linearized DNA template using *E. coli* bacteriophage T7 and T3 promoters located upstream of the polylinker site in the plasmid vector (promoter map sequence: Stratagene Cloning Systems, La Jolla, CA, Appendix). The transcription reaction was then carried out using radiolabeled uridine triphosphate and either T7 or T3 RNA polymerase.

The collagen type I cDNA (gift from B. Kream, Department of Medicine, School of Medicine, University of Connecticut Health Center) consisted of a 1600 base-pair fragment of rat collagen α1(I) strand inserted into pUC18 plasmid. The probe was made by excising the collagen I fragment with the restriction enzyme *PstI* and then labeling the fragment using the random primer method described above (11). The collagen type III cDNA (gift from D. Toman, Department of Molecular Genetics, University of Texas M.D. Anderson Cancer Center) consists of a 331 base-pair fragment of the *C*-terminal propeptide domain of mouse collagen III (α1) inserted into the Bluescript KS+ phagemid. The insert was excised from the vector using the restriction enzymes *BamHI* and *HinDIII* and used in a random priming transcription reaction to yield a radiolabeled probe. The prolyl 4-hydroxylase (P4-H) cDNA (gift from D. John, School of Biological Science, University of Manchester, UK) consisted of a rat clone containing the entire coding sequence of the α subunit of P4-H inserted into the Bluescript phagemid. After this template is linearized using *XbaI* restriction enzyme, a riboprobe was synthesized using T7 primer and T7 RNA polymerase. The transforming growth factor (TGF-β) probe was a partial cDNA clone (approximately 1 Kb) from the coding region of rat TGF-β inserted into Bluescript2 KS vector (American Type Culture Collection System, depositor S.W. Qian, Laboratory of Chemoprevention, Bethesda, MD) which was excised using the restriction enzyme *EcoRI.* A radiolabeled TGF-β probe was made using the random priming method. The GAPDH probe was a human GAPDH cDNA 1.2 Kb insert in a Bluescript SK vector. A random primed probe was made from this cDNA after excising the insert with *EcoRI* restriction enzyme.

Collagenase Assay

RV and LV samples were washed and immediately frozen at −70 °C. Zymography was performed as described by Tyagi et al. with modifications (37). At the time the assay was performed, 15 mg of sample was weighed and placed in ice cold extraction buffer (10 mM cacodylic acid, 0.15 M NaCl, 20 mM CaCl2, 0.01% Triton X-100). Following incubation overnight in extraction buffer at 4 °C with constant agitation, the samples were centrifuged and the supernatant was saved. The extraction was repeated with fresh extraction buffer. After adjusting the pH of the combined supernatants to 7.4 with 0.1 M Tris-HCl, the samples were concentrated to 0.5 ml using 15,000 MW cut-off concentrators (Minicon-B15, Amicon, Beverly, MA).

An aliquot of each sample was mixed 3:1 with sample buffer (10% SDS, 4% sucrose, 0.25 M Tris-HCl at pH 6.8, and 0.1% bromphenol blue) and loaded onto a 10% acrylamide denaturing gel containing 40 μg/ml rat tail collagen type I (150 × 145 × 1 mm) (16). Electrophoresis was carried out in a vertical flat-bed electrophoresis apparatus (R. Shadel, Inc., San Francisco, CA) for 3 hours at 25 mA at 4 °C. After electrophoresis, the gels were washed twice (15 minutes at room temperature) in 2.5% Triton X-100 then rinsed thoroughly in distilled water. The gels were incubated in substrate buffer (50 mM Tris-HCl pH 8.0, 5 mM CaCl2) 24 hours at 37 °C to allow the collagenase to degrade collagen in the gel. After incubation the gels were stained in 0.05% Coomassie Blue R-250 in acetic acid:isopropanol:water mixture (1:3:6) and destained in water. Destained gels were scanned (Quick Scan Jr., Helena Laboratories, Beaumont, TX) and the intensity was recorded. The percent decrease in intensity indicating the collagenase activity was calculated as 100 × (intensity of blank − intensity of sample)/ intensity of blank. Samples were all run in duplicate. Samples from one PA banded and one sham operated rat were run side-by-side on the same gel to control for differences in reaction efficiency and staining. Thus, collagenase activities were reported as the ratio of PA banded to sham.

As there was some variability in the zymography assay results, we used a second assay, the ninhydrin assay, to confirm the collagenase assay results mea-

sured with zymography. The ninhydrin collagenase assay is a colorimetric assay based on the detection of breakdown products of collagen using ninhydrin (13).

Statistics

Sham and PA banded right and left ventricular and skeletal muscle wet to dry ratios were compared using an ANOVA with a Fishers PLSD posthoc analysis. Collagen contents in ventricular myocardium and skeletal muscles were compared in the same manner using an ANOVA with a Fishers PLSD posthoc analysis. A one sample *t*-test was used to test whether the means of the ratios of PA banded to sham collagenase activity were different from unity. A nonparametric Mann Whitney U test was used to detect changes in collagen types I and III and prolyl 4-hydroxylase mRNA and TGF-β levels.

RESULTS

Body Weights and Heart Weights

Table 1 shows the average rat body weights (with standard deviations) in each group before surgery (prebanding BW) and at the time of sacrifice (postbanding BW). There was a small but significant difference in the weights of the PA banded rats banded for 7 days compared to the sham operated rats after 7 days (Table 1). This difference was detected in the prebanding weight and the weight when the rats were sacrificed. However, the average weight gain was not significantly different in the 7-day sham and PA banded rats. There were no other differences in the weights of the rats.

The ratios of right and left ventricular weights to prebanding body weights are also shown in Table 1. The ratio of RV weight to body weight increased significantly in the PA banded rats compared to sham operated rats. However, LV weight to body weight did not change significantly in the PA banded rats compared to sham rats. The ratio of ventricular to postbanding body weight was also calculated with similar results (data not shown).

Right Ventricular Pressures

RV pressure was measured to monitor the extent of PA banding (Table 2). Mean RVP before banding ranged from 9 mm Hg to 13 mm Hg. After PA banding the mean RVP ranged from 19 mm Hg to 22 mm Hg. Reanesthetization of PA banded rats one day post-op proved problematic, therefore, RVP measurements in this group were not made. At the time of sacrifice, the RVP in the PA banded group was still significantly elevated. In the sham operated rats, no significant differences were detected in the RVP at the time of sacrifice compared to the prebanding RVP.

Right and Left Ventricular Wet to Dry Ratios

In both the RV and the LV, the wet to dry ratios were significantly higher in the PA banded rats compared to the controls after only 1 day of pulmonary artery banding (Fig. 1). The wet to dry ratios remain significantly higher in the PA banded rats compared to sham operated rats after 3, 7, and 28 days of PA banding in both the RV and LV (Fig. 1).

Skeletal Muscle Wet to Dry Ratios

To see if edema development was a generalized phenomenon, we also measured wet to dry ratios in skeletal muscle at 7 and 28 days after PA banding or sham operation. In contrast to the wet to dry ratios in the heart, there is no significant difference in skeletal muscle (biceps pectoris) wet to dry ratios of PA banded and sham operated rats (Fig. 2).

Right and Left Ventricular Collagen Concentration

After determining the time course of edema development in the heart, we wanted to correlate these

Table 1. Average body weights and heart weights from sham and pulmonary artery banded rats

Protocol	Time after PA banding	Prebanding BW (g)	Postbanding BW (g)	Weight gain	RV weight/BW (mg/g)	LV weight/BW (mg/g)
Sham	1 day	351.3 ± 33.5	330.3 ± 44.7	−20.9 ± 7.9	0.512 ± 0.137	1.256 ± 0.320
	3 days	342.5 ± 22.0	320.5 ± 21.8	−18.1 ± 10.8	0.482 ± 0.070	1.255 ± 0.294
	7 days	366.4 ± 28.1	256.2 ± 25.7	−3.0 ± 14.4	0.515 ± 0.121	1.523 ± 0.200
	28 days	336.4 ± 32.2	375.3 ± 55.2	43.8 ± 34.2	0.609 ± 0.121	1.671 ± 0.356
PA banded	1 day	333.3 ± 21.7	302.8 ± 19.9	−24.9 ± 4.1	0.787 ± 0.176*	1.224 ± 0.134
	3 days	340.8 ± 32.5	315.6 ± 37.2	−29.1 ± 16.6	0.648 ± 0.229	1.156 ± 0.279
	7 days	338.1 ± 23.1*	323.5 ± 21.0*	−6.7 ± 13.6	0.682 ± 0.204	1.271 ± 0.333
	28 days	355.3 ± 29.4	394.1 ± 53.9	38.9 ± 54.0	0.965 ± 0.228*	1.549 ± 0.295

*$p < 0.05$ PA banded versus sham.

Table 2. Right ventricular pressures before and after pulmonary artery banding

Protocol	Time after PA banding	Prebanding RVP (mm Hg)	Postbanding RVP (mm Hg)	RVP at sacrifice (mm Hg)
Sham	1 day	10.7 ± 1.9	10.7 ± 1.9	10.2 ± 2.9
	3 days	11.3 ± 2.1	11.3 ± 2.1	11.3 ± 3.2
	7 days	10.0 ± 1.9	10.0 ± 2.0	11.8 ± 2.5
	28 days	10.4 ± 1.1	10.4 ± 1.1	10.4 ± 0.5
PA banded	1 day	10.3 ± 5.7	22.3 ± 4.7	—
	3 days	12.7 ± 4.6	19.2 ± 4.9	19.5 ± 0.7
	7 days	8.7 ± 1.9	22.0 ± 3.8	19.0 ± 1.4
	28 days	12.5 ± 2.8	22.0 ± 3.6	17.2 ± 4.5

changes with the development of myocardial interstitial fibrosis. In both the right and left ventricles, no significant changes in collagen content (g%) were detected 1 day or 3 days after pulmonary artery banding or sham operation (Fig. 3). However, at the 7-day and 28-day time points, total collagen content was significantly higher in the pulmonary artery banded rats compared to sham operated rats in both the right and left ventricles (Fig. 3). Approximately a 200% increase in collagen content in the RV and about a 50% increase in LV collagen content were detected 7 days after PA banding. Total baseline collagen content in the LV was lower than in the RV (LV collagen 1.74 ± 0.049 g%, RV collagen 2.70 ± 0.046 g % at 0 days). In the PA banded rats, a significant change in collagen content over time was measured in both the right and left ventricles. The increase in collagen content was greater in the RV (3.7-fold increase 0 vs. 28 days after PA banding) compared to the LV (2.5-fold increase 0 vs. 28 days after PA banding).

Skeletal Muscle Collagen Concentration

To determine if the increase in collagen content was specific to cardiac muscle, total collagen content was also measured in skeletal muscle (biceps femoris) at 7 days and 28 days after pulmonary artery banding or sham operation (i.e., when significant changes in collagen content in RV and LV tissue were detected). No significant differences in skeletal muscle total collagen content were found when comparing PA banded to sham operated rats (Fig. 4).

Collagen mRNA Levels

Figure 5 shows myocardial collagen types I and III mRNA levels following sham operation or PA banding. The mRNA levels represent a ratio of PA banded to sham mRNA levels at each time point. Thus, a ratio greater than one represents an increase in

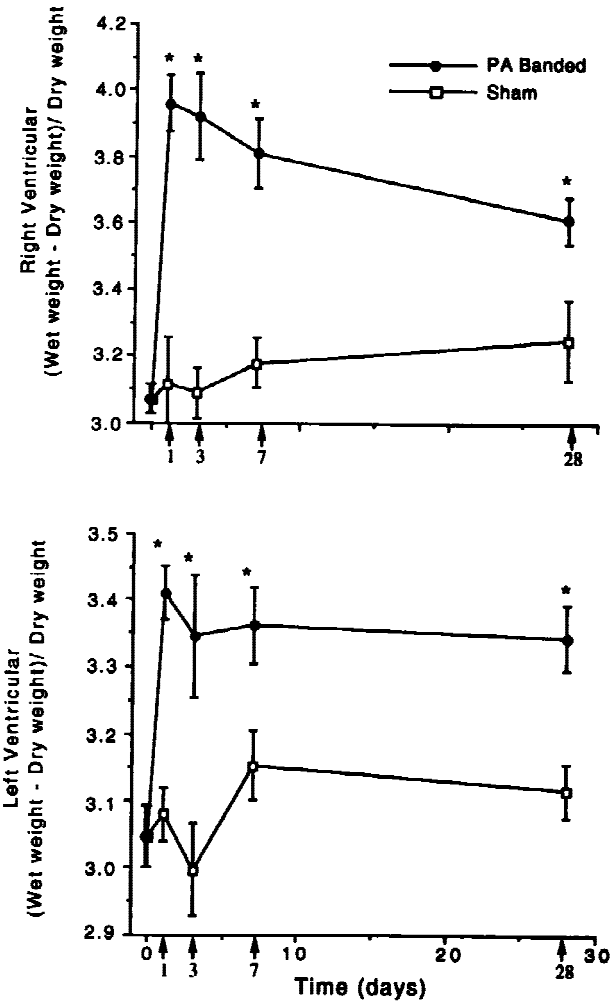

Figure 1. Right ventricular (upper panel) and left ventricular (lower panel) wet to dry ratios, indicating the amount of myocardial edema, are shown for PA banded rats (solid symbols) and sham operated rats (open symbols). Myocardial edema develops within 1 day and is sustained up to 28 days after surgery in the PA banded group but not the sham group. *$p < 0.05$ PA banded versus sham.

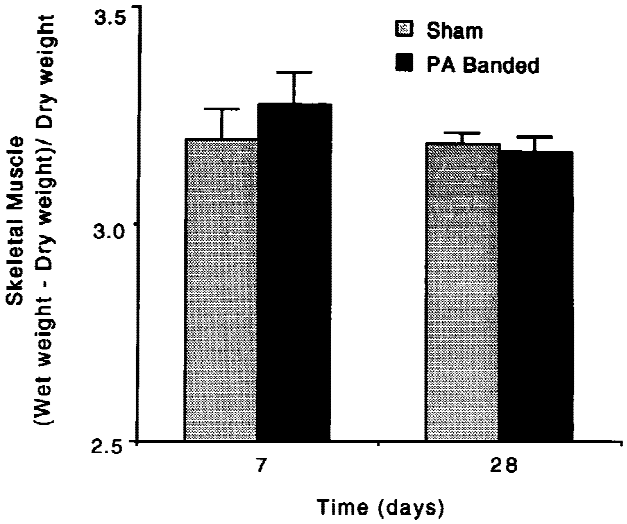

Figure 2. Skeletal muscle (biceps pectoris) wet to dry ratios indicating edema in sham (speckled bars) and PA banded (solid bars) rats are shown. No differences in wet to dry ratios were detected between PA banded and sham rats 7 or 28 days after surgery.

mRNA levels in the PA banded rats compared to shams.

No increase in collagen type I mRNA levels was detected one day after PA banding, and steady-state mRNA levels for collagen type I increased significantly in both the RV and LV compared to sham 3 days after PA banding. In the LV, collagen type I mRNA levels remained elevated while in the RV mRNA levels returned to near baseline. Similarly, collagen type III mRNA levels increased significantly in both the RV and LV 3 days after PA banding compared to sham operated rats. However, collagen type III levels remained elevated in the RV after 7 days of PA banding; whereas LV collagen type III mRNA levels in the PA banded group appeared to be elevated compared to shams but were not significantly different from sham levels 7 days after PA banding.

Prolyl 4-Hydroxylase Levels

Although we found increased collagen mRNA levels in PA banded rats indicating collagen synthesis, we wanted to determine if increased collagen processing also contributed to the increased myocardial collagen accumulation in PA banded rats compared to shams. Therefore, we measured mRNA levels for the α subunit of prolyl 4-hydroxylase, the enzyme catalyzing the hydroxylation of prolyl residues on collagen necessary for triple-helix formation of the collagen trimer. Figure 6 shows the ratio of prolyl 4-hydroxylase steady-state myocardial mRNA levels in PA banded and sham rats. Steady-state prolyl 4-hydroxylase increased significantly in the RV only 1 day after PA banding and remained elevated up to 3 days in PA banded rats compared to sham rats. Although prolyl 4-hydroxylase mRNA levels did not increase until 3 days after PA banding in the LV compared to 1 day in the RV, the prolyl 4-hydroxylase levels remained elevated at 7 days after PA banding in the LV, whereas RV mRNA levels decreased between 3 and 7 days after PA banding.

Transforming Growth Factor-β

TGF-β mRNA levels are expressed as the ratio of PA banded animals to sham operated animals and were compared using the nonparametric Mann Whitney U

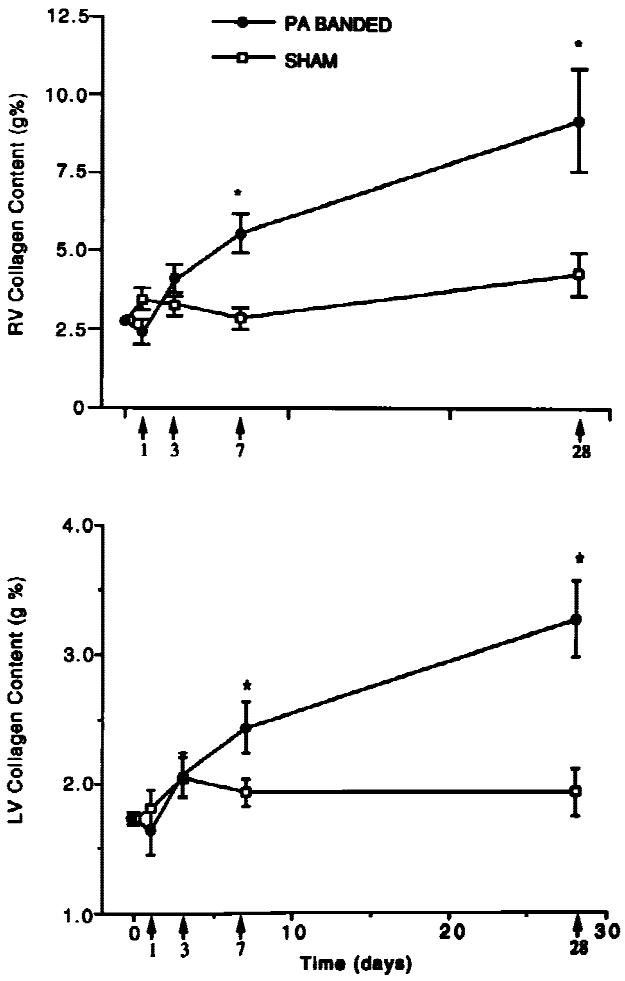

Figure 3. Right ventricular (upper panel) and left ventricular (lower panel) collagen content in PA banded (solid symbols) and sham (open symbols) rats are shown. Right and left ventricular collagen content increases significantly 7 days after surgery in the PA banded rats compared to the sham rats. *$p < 0.05$ PA banded versus sham.

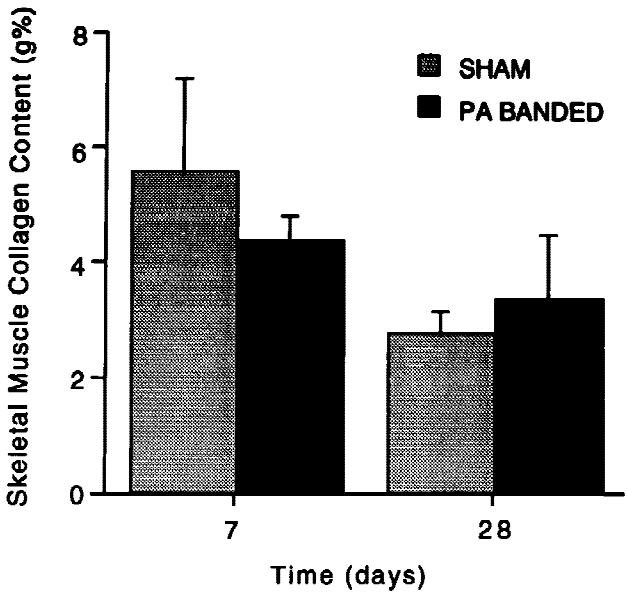

Figure 4. Skeletal muscle collagen content in sham (speckled bars) and PA banded (solid bars) rats are shown. No differences in the collagen content was detected between sham and PA banded rats.

test. The LV TGF-β ratios ranged from 1.89 ± 0.5 on day 1 to 2.6 ± 0.9 on day 3 while the RV TGF-β ratio ranged from 1.22 ± 0.25 on day 1 to 2.68 ± 0.5 on day 3. No statistical difference could be demonstrated in either the LV or RV.

Collagenase Activity

RV and LV collagenase activities measured by zymography are shown in Fig. 7. Data are expressed as a ratio of PA banded to sham in order to control for differences in reaction efficiency and staining. In the RV, the ratio of PA banded to sham collagenase activity 3 days after PA banding was significantly greater than 1 (i.e., collagenase activity was greater in the PA banded rats compared to sham rats). Although there was no significant differences in RV collagenase activity at 7 days of PA banding, collagenase activity tended to be lower in the PA banded rats compared to controls when measured with zymography. After 28 days of PA banding, RV collagenase activity tended to be greater in the PA banded rats compared to sham rats; however, this ratio was not significantly greater than 1.

LV collagenase activity in PA banded rats was significantly lower after 7 days of PA banding when compared to sham rats. Although LV collagenase activities after 3 and 28 days of PA banding tended to be lower in the PA banded rats compared to shams, these changes were not significant. The collagenase assay results were confirmed using the ninhydrin assay (data not shown).

DISCUSSION

To study the chronic effects of myocardial edema on cardiac fibrosis development, we utilized a chronic rat pulmonary artery banded model. This model allowed us to study the effects of edema on collagen metabolism in the LV independent of pressure overload and hypertrophic effects found in the RV. In

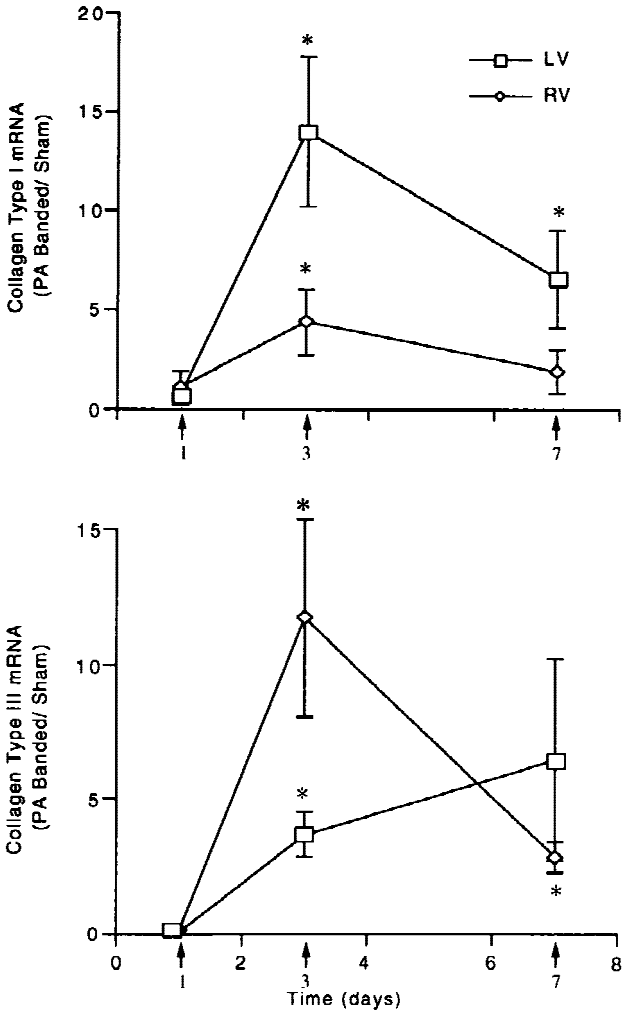

Figure 5. Collagen types I and III steady-state mRNA levels are shown in the upper and lower panels, respectively. The graphs show the ratio of PA to sham mRNA levels in the left ventricle (squares) and in the right ventricle (diamonds). Collagen type I mRNA levels increased significantly 3 days after PA banding in both the right and left ventricle. Collagen type III increased significantly 3 days after PA banding in the left ventricle and 7 days after PA banding in the right ventricle. *$p < 0.05$ PA banded versus sham.

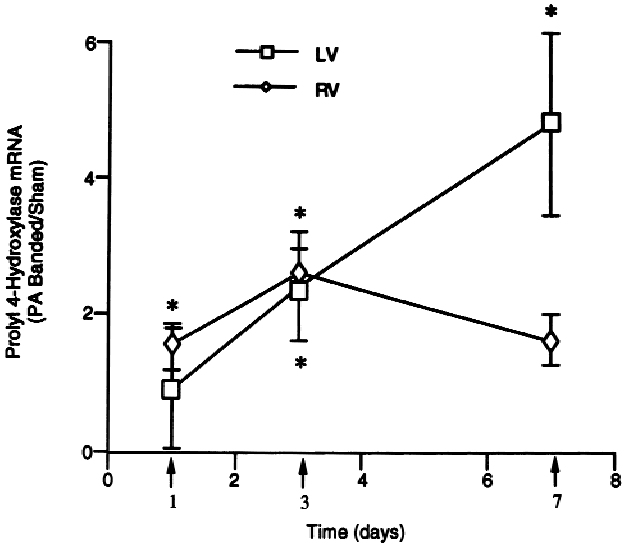

Figure 6. The ratios of PA banded to sham prolyl 4-hydroxylase α subunit steady-state mRNA levels at 1, 3, and 7 days after surgery are shown. RV prolyl 4-hydroxylase mRNA levels are significantly elevated 1–3 days after PA banding compared to sham rats. In the LV, prolyl 4-hydroxylase mRNA levels are elevated 3–7 days after PA banding. *$p < 0.05$ PA banded versus sham.

previous experiments using an acute dog model, we demonstrated that myocardial edema develops within 3 hours after PA banding. We confirmed these results in the rat model by demonstrating a significant increase in the wet to dry ratio 1 day after pulmonary artery banding in both the RV and LV compared to sham rats. We also showed that myocardial edema persists as long as PA pressures are elevated as demonstrated by increased LV and RV myocardial edema at 28 days after banding in our experimental group compared to shams. This data is supported by previous experiments in our laboratory in which LV myocardial edema was observed 6 months to 1 year after pulmonary artery banding in a canine model of pulmonary hypertension (17).

The early development of myocardial edema in pulmonary hypertension preceded the increased mRNA levels for collagen types I and III and prolyl 4-hydroxylase that occurred 3 days after PA banding. This is consistent with the hypothesis that edema may induce both increased synthesis of collagen and increased processing of collagen by prolyl 4-hydroxylase. Prolyl 4-hydroxylase is a tetramer consisting of two α and two β subunits (4). The β subunits are produced in excess; hence, it appears that the synthesis of the α subunit is the rate-limiting step in prolyl hydroxylase activity (4). Thus, increased prolyl 4-hydroxylase α subunit mRNA levels suggest increased synthesis of the α subunit. The increased mRNA levels for collagen and prolyl 4-hydroxylase were followed by increased myocardial collagen concentration 7 days after PA banding. In the left ventricle, this increased collagen concentration could be attributed to both an increase in collagen synthesis and processing and a decrease in collagen degradation by collagenase. In the right ventricle, collagen concentration increased despite increased collagenase activity and may be a result of RV hypertrophy not seen in the LV in our model.

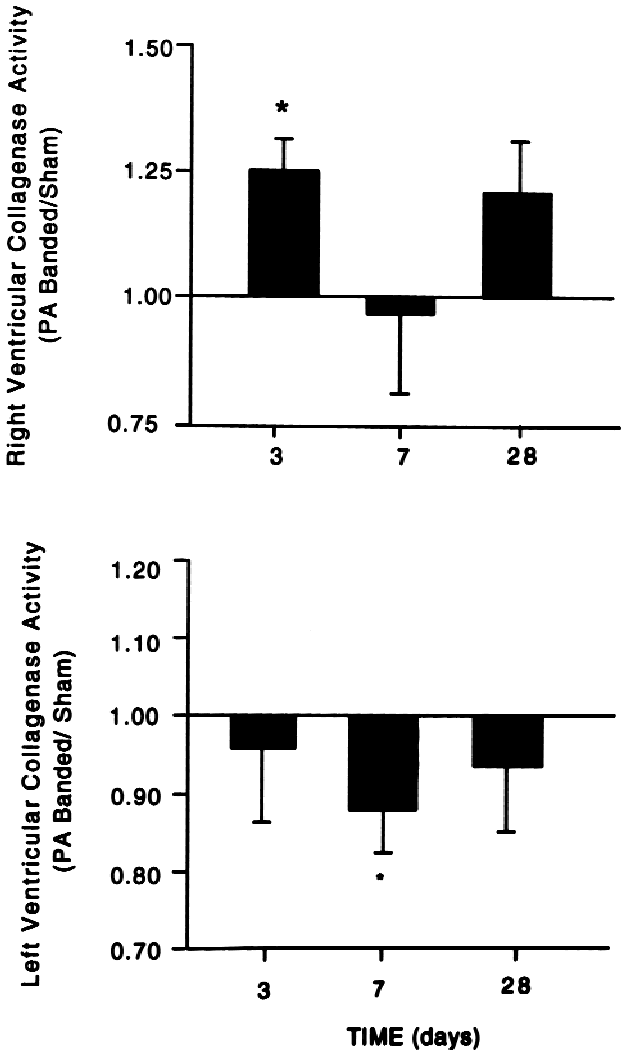

Figure 7. The ratios of PA banded to sham collagenase activity in the right (upper panel) and left (lower panel) ventricles are shown. While right ventricular collagenase activity increased significantly 3 days after PA banding, there was a significant decrease in left ventricular collagenase activity 7 days after PA banding. *$p < 0.05$ PA banded versus sham.

These data support the hypothesis that edema can trigger fibrosis development in pulmonary hypertension in several ways. First, the signal for fibrosis development occurred early in PH before collagen began to accumulate. We demonstrated that myocardial edema develops as early as 1 day after PA banding in our rat PH model as well as in a canine model of PH. Thus, edema development preceded cardiac fibrosis development. Second, as fibrosis was shown to develop in both ventricles in PH, the trigger for fibrosis development would also have to occur in both ventricles (6). We demonstrated that myocardial edema developed in both ventricles in our chronic PH model and thus may act as a signal for fibrosis development. Third, in our model, the LV was not subjected to pressure overload as in the RV, so the effects of edema could be studied independent of hemodynamic perturbations. Thus, we attributed LV fibrosis development to the presence of edema in the LV.

Data from other investigators support our findings. Miller and his colleagues studied the effects of chronic myocardial edema on fibrosis development in a chronic lymphatic obstruction model in the dog (23). When edema was produced in this model by repeated resection of the cardiac lymphatics for 3–16 weeks, endocardial thickening, due to increased fibrous and elastic tissue, was observed (23). Cardiac fibrosis also developed in a chronic lymphatic obstruction primate model (20). In both of these reports, fibrosis developed in the presence of myocardial edema and the absence of any hemodynamic perturbations.

We found several differences in collagen metabolism between the RV and LV. First, the collagen content increased more in the RV than in the LV. Second, collagenase activity increased in the RV but decreased in the LV. It should be noted that the septum was not included in analysis of the LV, therefore, changes in RV loading conditions were unlikely to influence LV collagen metabolism in this model. These interventricular differences may reflect increased RV load and subsequent RV hypertrophy compared to a normal load in the LV. We found increased RV weight to body weight ratios in the PA banded rats indicating the development of RV hypertrophy (Table 1). In addition to the pressure overload and hypertrophy, more edema developed in the RV compared to the LV. Thus, the higher RV collagen content may have been caused by more edema in the RV compared to the LV.

Although we have shown a correlative relationship between edema and fibrosis development, fibrosis development could be attributed to other causes. In addition to edema development, hormonal changes in response to pulmonary hypertension may affect the heart. Several investigators have proposed angiotensin II as the mediator of cardiac fibrosis development (41). While it is unclear whether angiotensin II is elevated in pulmonary hypertension (9), there is some evidence that angiotensin was not playing a role in our PH model. First, increased circulating angiotensin has been suggested to cause increased skeletal muscle collagen content as well as increased myocardial collagen content (30). In a study by Schieffer and coworkers, they found increased collagen content in skeletal muscle, which was attenuated with ACE inhibitors in a myocardial infarction rat model (30). In our model, we found no significant changes in skeletal muscle collagen content 28 days after PA banding. Second, in cardiac fibroblasts, increased angiotensin has been shown to induce increased TGF-β expression (24), which was not demonstrated in our study.

This study supports the hypothesis that edema may trigger fibrosis development in the heart in pulmonary hypertension; however, the mechanism by which chronic edema can trigger fibrosis development is less clear. As collagen is primarily produced by fibroblasts in the heart, edema must cause extracellular matrix remodeling by modulating the cardiac fibroblast phenotype. Edema may trigger fibrosis development through an increased interstitial hydrostatic pressure acting on the fibroblasts. Increased myocardial edema has been shown to cause increased interstitial hydrostatic pressure (19). In several cell types, increased hydrostatic pressure has been shown to increase the synthesis and secretion of collagen. For instance, lamina cibrosa cells (cells involved in the development of glaucoma), cultured in the presence of increased hydrostatic pressure, increased synthesis and secretion of collagen type I (46).

Increased stretch induces extracellular matrix remodeling in fibroblasts (7). Increased hydrostatic pressure has been shown to induce endothelial cells to release basic fibroblast growth factor and to cause changes in plasma membrane properties in fibroblasts (1,15,45). It is clear that fibroblasts are able to respond to changes in hydrostatic pressure.

The effects of hydrostatic pressure on fibroblasts may be transduced by integrins on the fibroblast cell surface. Hydrostatic pressure has been shown to

modulate cell–matrix attachment in endothelial cells (36). An increase in extracellular fibronectin fibers and fibronectin receptors were observed when bovine aortic endothelial cells were exposed to increased hydrostatic pressure (36). Thus, in endothelial cells, increased hydrostatic pressure increased cell–matrix attachments through integrin–fibronectin attachments.

Edema may alter cell–matrix interactions through increased hydrostatic pressure or by other mechanisms such as increasing intercellular distance. In fibroblasts, integrin-mediated cell–matrix interactions have been shown to be involved in modulating extracellular matrix properties. For instance, interruption of integrin-mediated interactions between human gingival fibroblasts and extracellular collagen contributed to fibrosis development (8). Thus, edema may modulate the extracellular matrix by altering integrin-mediated fibroblast–matrix interactions.

In summary, this study supports the hypothesis that edema triggers myocardial interstitial fibrosis development in pulmonary hypertension. We have shown that edema develops within hours after pulmonary artery banding and is followed by increased collagen synthesis through increased collagen types I and III mRNA levels and increased collagen processing. In the LV, the collagen concentration is increased in the absence of any hemodynamic changes. Thus, the increased collagen concentration can be attributed to the presence of LV interstitial edema. Understanding the relationship between chronic myocardial edema, interstitial fibrosis, and compromised cardiac function may lead to interventions designed to minimize the negative impact of these factors.

ACKNOWLEDGMENTS

The authors thank Ira Lown and Edwin Ostrin for their excellent technical assistance.

REFERENCES

1. Acevedo AD, Bowser SS, Gerritsen ME, Bizios R. (1993). Morphological and proliferative responses of endothelial cells to hydrostatic pressure: role of fibroblast growth factor. *J Cell Physiol* 157(3):603–614.
2. Alwine JC, Kemp DJ, Stark GR. (1977). Method for detection of specific RNAs in agarose gels by transfer to diazobenzyloxymethyl-paper and hybridization with DNA probes. *Proc Natl Acad Sci USA* 74:5350–5354.
3. Berg RA. Determination of 3- and 4-hydroxyproline. (1982). *Meth Enzymol* 82:372–399.
4. Berg RA, Kao WW, Kedersha NL. (1980). The assembly of tetrameric prolyl hydroxylase in tendon fibroblasts from newly synthesized alpha-subunits and from preformed cross-reacting protein. *Biochem J* 189(3):491–499.
5. Brilla CG, Pick R, Tan LB, Janicki JS, Weber KT. (1990). Remodeling of the rat right and left ventricles in experimental hypertension. *Circ Res* 67:1355–1364.
6. Buccino RA, Harris E, Spann JF, Sonnenblick EH. (1969). Response of myocardial connective tissue to development of experimental hypertrophy. *Am J Physiol* 216(2):425–428.
7. Carver W, Nagpal ML, Nachtigal M, Borg TK, Terracio L. (1991). Collagen expression in mechanically stimulated cardiac fibroblasts. *Circ Res* 69:116–122.
8. Chou DHI, Lee W, McCulloch CAG. (1996). TNF-α inactivation of collagen receptors. Implications for fibroblast function and fibrosis. *J Immunol* 156:4354–4362.
9. Cordoso PF, Hsieh CM, Daniel L, Yokomise H, Kato H, Strangemore BL, Miller JD, Logan AG, Radowski H, Patterson GA, Blendis LM. (1991). Plasma atrial natriuretic factor concentrations in a canine model of right heart pressure overload. *Clin Invest Med* 14: 310–319.
10. Davis KL, Mehlhorn U, Laine GA, Allen SJ. (1995). Myocardial edema, left ventricular function and pulmonary hypertension. *J Applied Physiol* 78:132–137.
11. Feinberg AP, Vogelstein B. (1983). A technique for radiolabeling DNA restriction endonuclease fragments to high specific activity. *Anal Biochem* 132:6.
12. Glisin V, Crkvenjakov R, Byus C. (1974). Ribonucleic acid isolated by cesium chloride. *Biochemistry* 13: 2633–2637.
13. Harding VJ, Warneford FHS. (1916). The ninhydrin reaction with amino-acids and ammonium salts. *J Biol Chem* 25:319–322.
14. Kohama A, Tanouchi J, Hori M, Kitabatake A, Kamada T. (1990). Pathologic involvement of the left ventricle in chronic cor pulmonale. *Chest* 98:794–800.
15. Kolpokov V, Rekhter MD, Gordon D, Wang WH, Kulik TJ. (1995). Effect of mechanical forces on growth and matrix protein synthesis in the in vitro pulmonary artery. Analysis of the role of individual cell types. *Circ Res* 77:823–831.
16. Laemmli UK. (1970). Cleavage of structural proteins during the assembly of the head of bacteriophage T4 *Nature* 227:680–685.
17. Laine GA, Allen SJ. (1991). Left ventricular myocardial edema. Lymph flow, interstitial fibrosis, and cardiac function. *Circ Res* 68:1713–1721.
18. Laine GA, Allen SJ, Katz J, Gabel JC, Drake RE. (1987). Outflow pressure reduces lymph flow rates from various tissues. *Microvasc Res* 33:135–142.
19. Laine GA, Granger HJ. (1985). Microvascular, interstitial, and lymphatic interactions in normal heart. *Am J Physiol* 249:H834–H842.

20. McKinney B. (1976). Endocardial changes produced in Patus monkeys by the ablation of cardiac lymphatics and the administration of a plantain diet. *Am Heart J* 91: 484–491.
21. Mehlhorn U, Davis KL, Burke EJ, Adams D, Laine GA, Allen SJ. (1995). Impact of cardiopulmonary bypass and cardioplegic arrest on myocardial lymphatic function. *Am J Physiol* 268:H178–H183.
22. Miller AJ, Pick R, Katz LN. (1960). Ventricular endocardial pathology produced by chronic cardiac lymphatic obstruction in the dog. *Circ Res* 8:941–947.
23. Miller AJ, Pick R, Katz LN. (1963). Ventricular endomyocardial changes after impairment of cardiac lymph flow in dogs. *Br Heart J* 25:182–190.
24. Moriguchi Y, Matsubara H, Mori Y, Murasawa S, Masaki H, Maruyama K, Tsutsumi Y, Shibasaki Y, Tanaka Y, Nakajima T, Oda K, Iwasaka T. (1999). Angiotensin II-induced transactivation of epidermal growth factor-b synthesis via transcriptional and posttranslational mechanisms. *Circ Res* 84:1073–1084.
25. Narayan S, Janicki JS, Shroff SG, Pick R, Weber KT. (1989). Myocardial collagen and mechanics after preventing hypertrophy in hypertensive rats. *Am J Hypertens* 2: 675–682.
26. Pearce M, Yamashita J, Beazell J. (1962). Measurement of pulmonary edema. *Circ Res* 16:482–488.
27. Pearlman ES, Weber KT, Janicki JS, Pietra GG, Fishman AP. (1982). Muscle fiber orientation and connective tissue content in the hypertrophied human heart. *Lab Invest* 46:158–164.
28. Pratt JW, Schertel ER, Schaefer SL, Esham KL, McClure DE, Heck CF, Myerowitz PD. (1996). Acute transient coronary venous hypertension impairs left ventricular function and induces myocardial edema. *Am J Physiol* 271(3 pt. 2):H834–H841.
29. Rohn DA, Davis KL, Mehlhorn U, Allen SJ, Laine GA. (1995). Myocardial edema and compromised left ventricular function attributable to difilariasis and cardiopulmonary bypass in dogs. *Am J Vet Res* 56: 221–226.
30. Schieffer B, Wollert KC, Berchtold M, Saal K, Schieffer E, Hornig B, Riede UN, Drexler H. (1995). Development and prevention of skeletal muscle structural alterations after experimental myocardial infarction. *Am J Physiol* 269:H1507–H1513.
31. Shirani J, Pick R, Guo Y, Silver MA. (1992). Usefulness of the electrocardiogram and echocardiogram in predicting the amount of interstitial myocardial collagen in endomyocardial biopsy specimens of patients with chronic heart failure. *Am J Cardiol* 69(17): 1502–1503.
32. Sullivan MJ. (1995). Congestive heart failure: trends in epidemiology and therapy. In: *Congestive Heart Failure. Current Clinical Issues.* (GT Kennedy and MH Crawford, eds.) Futura Publishing Company, Inc., New York, pp. 1–16.
33. Szidon JP. (1989). Pathophysiology of the congested lung. *Cardiol Clinics* 7:39–48.
34. Tabor S, Richardson CC. (1985). A bacteriophage T7 RNA polymerase/promoter system for controlled exclusive expression of specific genes. *Proc Natl Acad Sci USA* 82:1074–1078.
35. Tazelaar HD. (1992). Pathology of cardiac transplantation: recipient hearts (chronic heart failure) and donor hearts (acute and chronic rejection). *Mayo Clin Proc* 67:685–696.
36. Thoumine O, Nerem RM, Girard PR. (1995). Oscillatory shear stress and hydrostatic pressure modulate cell–matrix attachment proteins in cultured endothelial cells. *In Vitro Cell Dev Biol* 31:45–54.
37. Tyagi SC, Ratajaska A, Weber KT. (1993). Direct extraction and estimation of collagenase(s) activity by zymography in microquantities of rat myocardium and uterus. *Clin Biochem* 26:191–198.
38. Ullal SR, Kluge TH, Gerbode F. (1972). Functional and pathologic changes in the heart following chronic cardiac lymphatic obstruction. *Surgery* 71:328–334.
39. Ullrich A, Shine J, Chirgwin J, Pictet R, Tischer E, Rutter WJ, Goodman HM. (1977). Rat insulin genes: construction of plasmids containing the coding sequences. *Science* 196:1313–1319.
40. Unverferth DV, Baker PB, Swift SE, Chaffee R, Fetters JK, Uretsky BF, Thompson ME, Leier CV. (1986). Extent of myocardial fibrosis and cellular hypertrophy in dilated cardiomyopathy. *Am J Cardiol* 57:816–820.
41. Weber KT, Janicki JS, Shroff SG, Pick R, Chen RM, Bashey RI. (1988). Collagen remodeling of the pressure-overloaded, hypertrophied non-human primate myocardium. *Circ Res* 62:757–765.
42. Wegria R, Zekert H, Walter R, Entrup R, Schryvr C, Kennedy W, Paiewonsky D. (1963). Effect of systemic venous pressure on drainage of lymph from thoracic duct. *Am J Physiol* 204:284–288.
43. Williams J, Laine GA, Hanley E, Eberlein D, Sweeney M. (1990). Myocardial interstitial changes in humans with congestive cardiomyopathy. Abstract. *Anesth Analg* 70:S435.
44. Witte CL, Witte MH, Dumont AE. (1984). Pathophysiology of chronic edema, lymphedema, and fibrosis. In: *Edema*. (NC Staub and AE Taylor, eds.) Raven Press, New York, pp. 521–542.
45. Wright MO, Stockwell RA, Nuki G. (1992). Response of plasma membrane to applied hydrostatic pressure in chondrocytes and fibroblasts. *Connect Tissue Res* 28:49–70.
46. Yang JL, Neufeld AH, Zorn MB, Hernandez MR. (1993). Collagen type I mRNA levels in cultured human lamina cribrosa cells: effects of elevated hydrostatic pressure. *Exp Eye Res* 56:567–574.